

Airborne measurements in the longwave infrared using an imaging hyperspectral sensor

Jean-Pierre Allard, Martin Chamberland, Vincent Farley¹, Frédérick Marcotte, Matthias Rolland, ,
Alexandre Vallières, and André Villemaire
Telops inc., 100-2600 St-Jean-Baptiste, Québec, Qc, Canada G2E 6J5

ABSTRACT

Emerging applications in Defense and Security require sensors with state-of-the-art sensitivity and capabilities. Among these sensors, the imaging spectrometer is an instrument yielding a large amount of rich information about the measured scene. Standoff detection, identification and quantification of chemicals in the gaseous state is one important application. Analysis of the surface emissivity as a means to classify ground properties and usage is another one. Imaging spectrometers have unmatched capabilities to meet the requirements of these applications.

Telops has developed the FIRST, a LWIR hyperspectral imager. The FIRST is based on the Fourier Transform technology yielding high spectral resolution and enabling high accuracy radiometric calibration. The FIRST, a man portable sensor, provides datacubes of up to 320x256 pixels at 0.35mrad spatial resolution over the 8-12 μm spectral range at spectral resolutions of up to 0.25cm^{-1} . The FIRST has been used in several field campaigns, including the demonstration of standoff chemical agent detection [<http://dx.doi.org/doi.number.goes.here>]. More recently, an airborne system integrating the FIRST has been developed to provide airborne hyperspectral measurement capabilities. The airborne system and its capabilities are presented in this paper.

The FIRST sensor modularity enables operation in various configurations such as tripod-mounted and airborne. In the airborne configuration, the FIRST can be operated in push-broom mode, or in staring mode with image motion compensation. This paper focuses on the airborne operation of the FIRST sensor.

Keywords: airborne, hyperspectral imaging, imaging FTS, FTIR, standoff detection, remote sensing, thermal infrared, LWIR

1. INTRODUCTION

In addition to their consecrated role in fundamental research, recent developments have made it possible to miniaturize and ruggedize FTIR spectrometers to enable their use for many challenging field applications. In particular, the utilization of imaging FTIR spectrometers, such as the Telops FIRST, for passive remote sensing has proven to yield invaluable information about the scenes under investigation. Indeed, with their ability to measure the characteristic ways in which materials emit, scatter, transmit, absorb and reflect light, imaging FTIR spectrometers are ideally suited for the detection, classification and identification of chemical species. This powerful spectrometric tool is becoming more common in civil applications such as search and rescue, geological surveys, pollution monitoring, forest fires and combustion studies. These sensors are now also emerging as indispensable assets for defence operations through the role they can play for troops protection against chemical attacks, detection of mines and unexploded ordnances (UXOs) and for the localization of camouflaged targets.

Telops has developed the FIRST, a man-portable hyperspectral imager based on Fourier transform technology. This sensor offers a balanced combination of sensitivity, spatial, spectral and temporal resolutions. It has proven its dependable performance, robustness and effectiveness as a standoff chemical agent detector in numerous field campaigns. Until recently, the FIRST has been used in ground applications but its versatility allows extending its potential use to airborne measurements. This paper exposes the development of the FIRST-airborne system.

A summarized description of the FIRST is given in Section 2. Next, the design considerations of the FIRST-airborne system are presented in Section 3. Finally, the performances and capabilities of the airborne sensor are discussed in

¹ vincent.farley@telops.com; phone (418) 864-7808; fax (418) 864-7843; www.telops.com

Section 4. Particularly, the question of the dependency of the achievable NESR, spectral and spatial resolutions with respect to experimental parameters is addressed.

2. FIRST-LW SENSOR DESCRIPTION

The FIRST-LW is a lightweight and compact imaging radiometric spectrometer. The spectra measurements are performed using a Fourier-Transform Spectrometer (FTS). It uses a 320x256 LWIR PV-MCT focal plane array detector that can be windowed and formatted to fit the desired size and to decrease the acquisition time. Spectral resolution is user selectable and ranges from 0.25 to 150 cm^{-1} , with optimal system designed for 4 cm^{-1} . This instrument generates a complete spectrum of each pixel in the image, each pixel having an instantaneous field-of-view of 0.35 mrad. This field-portable sensor is shown in Figure 1.

The instrument has 2 internal calibration blackbodies used to perform an end-to-end radiometric calibration of the infrared measurements. In its longwave IR version, the instrument has sensitivity over the 8-12 μm band. This spectral band is ideal for passive standoff chemical agent detection at ambient temperatures. The sensor also has advanced acquisition and processing electronics, including 4 GB of high-speed DDR-SRAM, with the capability to convert the raw interferograms into spectra using real-time Discrete-Fourier Transform (DFT).



Figure 1: Picture of the FIRST, a LWIR hyperspectral imager

The control software has a user-friendly interface and provides real-time feedback to the operator. A screenshot of the control software (named FTPro) is presented in Figure 2. On the right, the non-uniformity corrected broadband IR image is displayed with a greyscale code where black means low radiance level and white high radiance level. The uncalibrated raw spectrum (or the interferogram as selected by the operator) of a selected pixel in the image is displayed in real time on the left of the screen. Additional key parameters such as the blackbodies temperature, the sensor temperature and the level of signal on the FPA are also displayed. Additional monitored values can be viewed in a separate panel. This main panel of the user interface is used to start the acquisition of the data or to initiate calibration measurements. The configuration of the sensor (image size and location, spectral resolution, blackbody and sensor temperature, etc...) is performed in another input panel. The sensor has the capability to change the focus of the IR image to produce a clear image at almost any distance from 3 meters up to infinity.

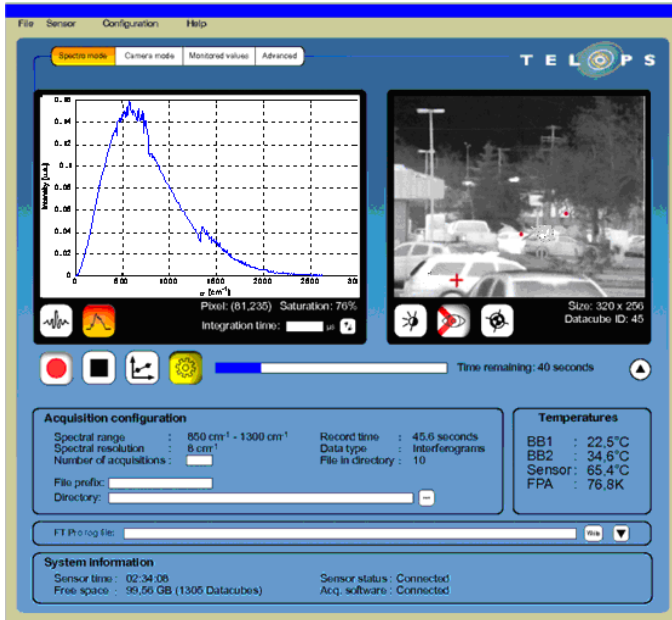


Figure 2: FTPro gives the operator real-time feedback, including the broadband IR image and the spectrum of a selected pixel

The FIRST was presented in detail in previous papers [1, 2]. It has been successfully used during several field trials.

3. DESIGN OF THE AIRBORNE CONFIGURATION

3.1 Design considerations

Before it is transformed into a spectrum, the data acquired by a FTS is initially an interferogram. It is required that all the samples in the interferogram be acquired from a stationary scene; otherwise the Fourier transform generates errors in the spectrum. In an airborne configuration, staring at a fixed scene can become a challenge, especially for high resolution spectra, that require long interferograms. The difficulty is primarily caused by the aircraft displacement, but it also originates from the plane variations in the yaw, pitch and roll orientations.

From this point, one can consider two options to address the stationary scene requirement:

- 1- Reduce acquisition parameters, such as the image size and the spectral resolution, in order to minimize the interferogram acquisition period and thus become less sensitive to aircraft displacement and angular movement.
- 2- Stare at the same ground area by using an image motion compensation (IMC) mirror that compensates the aircraft displacement and its angular movement.

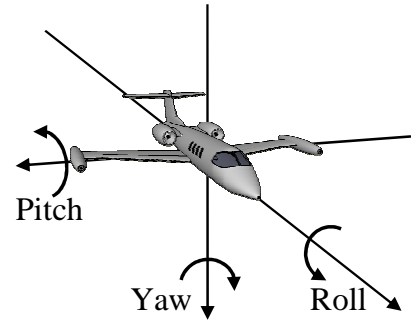


Figure 3. Airplane angular orientations

The second method is preferred, as it enables better spectral resolution. Figure 4 depicts the acquisition routine of a configuration where the instrument viewing angle compensates for the aircraft displacement. By using the IMC mirror, one can acquire large 2-D images that cover several pixel lines. Also, in order to facilitate the eventual mosaicking of the different ground sections, one can adjust its scanning parameters in order to allow consecutive images to overlap.

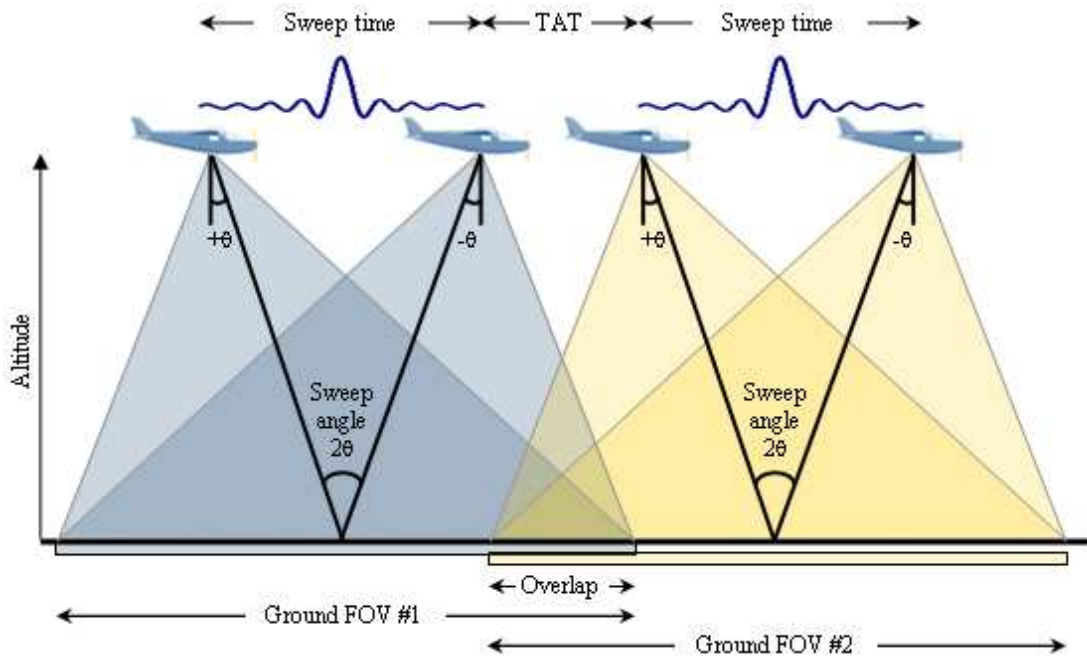


Figure 4. Interferogram acquisition in airborne configuration

The different abbreviations are defined as followed:

- $+\theta$ and $-\theta$: Initial and final IMC viewing angles
- Sweep time: Function of speed, altitude and sweep angle
- TAT : IMC mirror sweep reversal time, from $-\theta$ to $+\theta$

Small geometrical distortions of the pixel grid projected on the ground are inevitable during image motion compensation. We have chosen the initial (and final) IMC viewing angles so as to minimize the smearing effect below the acceptable level of one quarter of a pixel. With this objective, it has been found that the IMC viewing angles should be kept within $\pm 1^\circ$. As shown in Figure 5, the grid distortion is very low, even for corner pixels. The average pixel smear in this case is 0.2 pixel. In actual flight scenarios, only a portion of the FPA is used, making the analysis presented here a worse case.

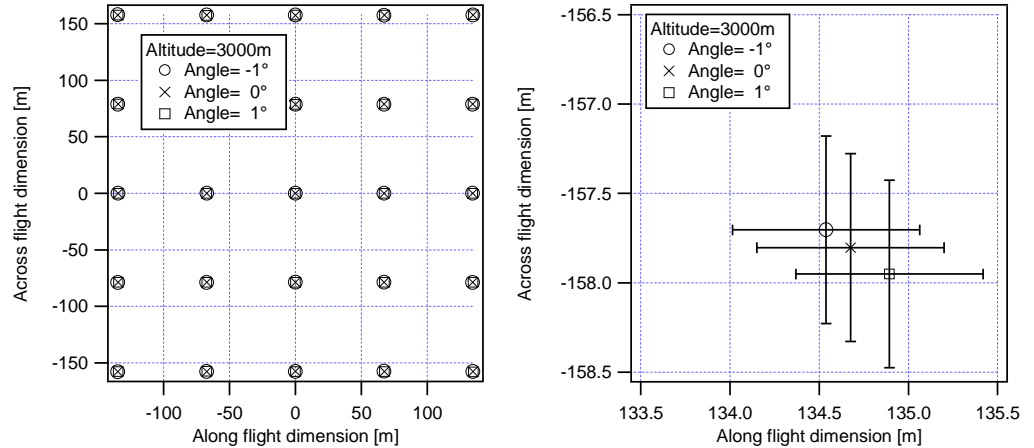


Figure 5. Projected pixels during IMC correction at an altitude of 3000m for the complete array (left) and zoom on the lower right pixel (right). In the graph on the right hand side, the error bars illustrate the extent of the pixel.

3.2 System configuration

The FIRST airborne system comprises the FIRST instrument along with several modules. The primary function of the assembly is to compensate for the aircraft displacement and its angular pitch, roll and yaw. It also adds accurate aircraft position and attitude data to the acquisition file metadata in order to later georeference the acquired data. The following section describes the role of each subsystem to fulfill the flight requirements.

In order to acquire the most useful infrared spectral ranges, the Telops airborne system allows mounting two different FIRST instruments. The FIRST-MW covers from 3 to 5.5 μ m whereas the FIRST-LW covers the 8 to 11.5 μ m wavelength range. The optical bench includes a stabilization platform, the two FIRST instruments, two IMC mirrors, a GPS/INS unit and two visible boresight cameras. All these modules are rigidly mounted on a high stiffness base plate. Figure 6 illustrate the FIRST airborne configuration.

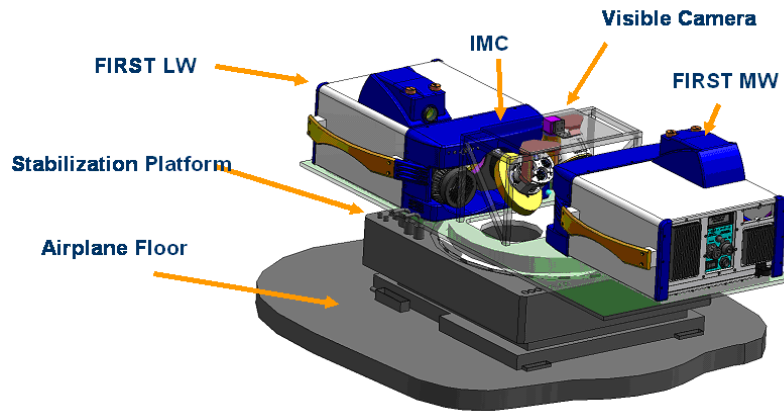


Figure 6. Illustration of the Airborne Configuration with 2 FIRST

3.3 Airborne stabilization platform

The stabilization platform has two functions: it dampens the aircraft vibrations and it compensates for the aircraft yaw. The roll and pitch are corrected by the IMC mirrors, see Section 3.4.

The yaw is corrected using the GPS/INS feedback. This platform configuration allows a rapid and precise correction for payloads with a moment of inertia up to 15 kg m². The platform is also equipped with vibration dampers. These dampers filter and minimize the effect of high frequency vibrations caused by the aircraft motors and the airflow around the aircraft fuselage.

The yaw correction is performed by interfacing the GPS/INS and the stabilization platform. The GPS/INS measures yaw errors with respect to flight direction. This information is applied as a correction to the Stabilization Platform. Figure 7 represents this process.

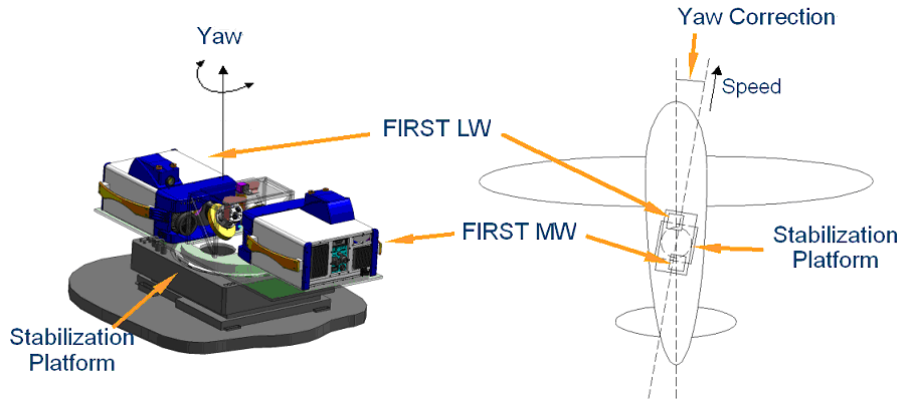


Figure 7. Yaw Correction

3.4 IMC mirrors

The IMC mirror is a rapid, two axes mirror:

- 1- In X, it cancels the aircraft pitch and it moves along the flight direction to compensates the aircraft displacement;
- 2- In Y, it cancels the aircraft roll.

The image motion compensation mirrors are fast steering mirrors based on a voice coil actuator design.

Figure 8 illustrates this subsystem. The image motion compensation mirror is optimized in order to minimize weight and response time.

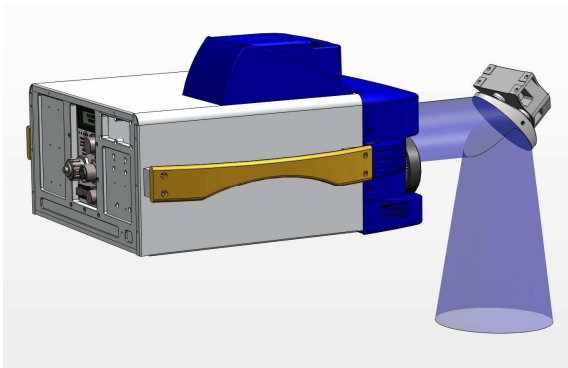


Figure 8. IMC mirror

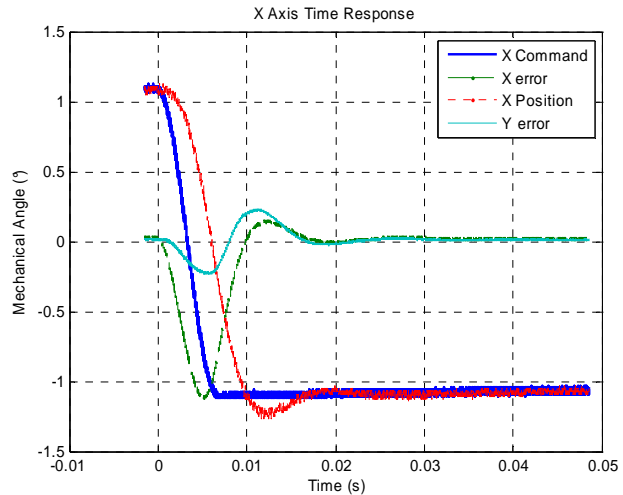


Figure 9. Typical IMC Performance for a command along the X-axis

The image motion compensation mirrors feature a retrace time typically around 20 msec as shown in Figure 9. The retrace time is the time required to return to the origin angle at the end of the acquisition cycle.

The roll and pitch are corrected by the IMC mirrors independently for each FIRST. Each IMC mirror is controlled by a video tracker electronic board. The video tracker receives a video stream coming from a visible camera installed on the FIRST instrument. At each acquisition start, the video tracker is triggered to record the current image as the reference. It then automatically identifies areas with sufficient contrast (see Figure 10). Then, the video tracker continuously provides the displacement of the last image from the reference scene in X and in Y. This information is analyzed by a digital signal processor (DSP) that is also providing feedback to the IMC mirror. Moreover, the aircraft angular orientations, provided by the GPS/INS at a faster rate than the video tracker error feedback, are also used as predictive information in the DSP algorithm to control the IMC mirror.

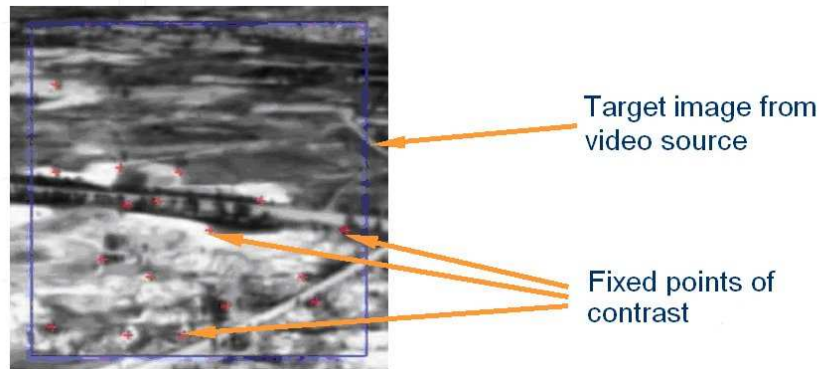


Figure 10. Target image used by the video tracker

3.5 GPS/INS

A GPS/INS module is used to geo-reference the acquisition and to assist the IMC mirror servo-loop, using the pitch and the roll measurements. The GPS/INS delivers the pitch, roll and yaw angle at a rate of 200Hz whereas the video tracker feedback rate is 60Hz. During the flight, the used mode is the C/A GPS (4-6m accuracy). This mode of operation does not require any other equipment or resources. Optionally the DGPS mode, which requires a nearby ground-based station, can be used to increase the spatial accuracy in post-processing.

The ground GPS position of each acquired scene is calculated using a triangulation technique. This technique uses the aircraft GPS position and the angles of the IMC mirror. After the ground GPS position is calculated, it is transferred to the FIRST in the metadata portion of the acquired file. The triangulation technique is illustrated in Figure 11.

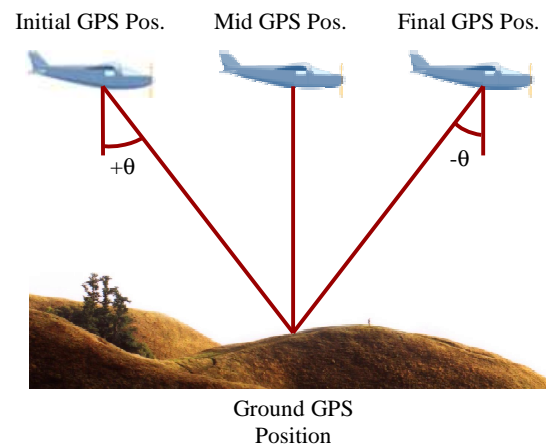


Figure 11. Ground GPS position calculated by the triangulation technique

4. AIRBORNE PERFORMANCES

FIRST performances have been extensively studied and discussed in previous papers [1, 2]. In this section, we address additional constraints inherent to the airborne utilisation of this hyperspectral imager. The spectral resolution, spatial resolution and Noise Equivalent Spectral Radiance (NESR) are interrelated through their dependency on the acquisition time of a datacube (or sweep time) and on flight conditions such as altitude and aircraft speed. Moreover, in order to obtain quality spectral data, smear effects must be minimized.

4.1 Performances criteria definitions

4.2 Spectral Resolution

In Fourier Transform Spectrometers (FTS), spectral resolution is a function of the Maximum Path Difference (MPD) of the interferogram. Telops defines spectral resolution (R_{FWHM}) with the Full-Width Half Maximum (FWHM) of the instrument lineshape as described in equation 1.

$$R_{FWHM} = \frac{1.2}{2 \cdot MPD} \quad [1]$$

This relation clearly states that spectral resolution improves as MPD increases. In the following discussion, it is assumed that the moving mirror of the interferometer moves at a constant speed. The maximum achievable MPD can thus equivalently be interpreted in terms of maximum available time for the moving mirror to complete a sweep. In this paper, this parameter is referred as the maximum sweep time. Consequently, all factors that limit sweep time will also restrict spectral resolution. As will shortly be explained, the spectral resolution of the FIRST-airborne is limited by flight conditions (aircraft speed and altitude) and by the interferometer metrology sampling period.

4.3 NESR

As its name indicates, the noise equivalent spectral radiance (NESR) is the total amount of noise of a spectroradiometer per spectral bin expressed in units of radiance. This performance parameter is of the outmost importance since it relates directly to the instrument sensitivity.

In FTS, sources of noise are diverse but can be categorized in one of four categories: electronics noise, detector sensitivity, instrument optical efficiency and acquisition settings. In this paper, the acquisition settings that impact the NESR are addressed. Equation 2 states that NESR is inversely proportional to spectral resolution.

The dependency of NESR to the total acquisition time (τ) indicates that increasing τ improves the NESR. An easy way to increase τ is to adjust the integration time of the focal plane array (FPA). Since the total acquisition time in airborne applications is limited by flight conditions, doing so means that fewer points can be acquired in each interferogram. Increasing integration time thus results in further limitations to sweep time and, consequently, to spectral resolution.

$$NESR \propto \frac{1}{R_{FWHM} \sqrt{\tau}} \quad [2]$$

4.4 Spatial resolution

When the optical blur is smaller than the size of a pixel, spatial resolution can be defined in terms of instantaneous Field-Of-View (iFOV), the angle subtended by a pixel. For most applications though, it is more natural to view spatial resolution in terms of dimension covered by a pixel. The FIRST possesses an iFOV of 0.35 mrad. In the airborne application, the angular iFOV ($iFOV_{\theta}$) is related to its spatial counterpart ($iFOV_{ground}$) through the altitude of the aircraft (see equation 3).

$$iFOV_{ground} = 2 \cdot Altitude \cdot \tan\left(\frac{iFOV_{\theta}}{2}\right) \quad [3]$$

The result of this equation is illustrated on Figure 12 for FIRST-airborne typical flight altitudes. As can be seen, the hyperspectral imager offers high spatial resolutions. One could be tempted to fly as low as possible in order to obtain the best spatial resolution but, as it is discussed in section 0, a gain in spatial resolution is done at the expense of spectral resolution and ground coverage.

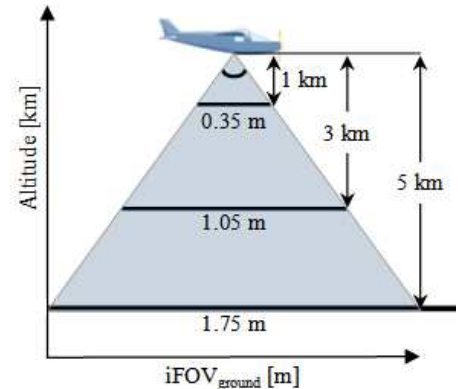


Figure 12. Spatial resolution vs altitude

4.5 Sampling distance and spectral range effects

In order to yield accurate spectra, the Optical Path Difference (OPD) at which the interferogram points are acquired must be precisely known. This is achieved by measuring the displacement of the interferometer moving mirror with an appropriate metrology system.

The FIRST metrology system is formed of a modulated HeNe laser beam. Since the light source is monochromatic, a sinusoidal shaped signal results from this modulation. Usually, the scene interferogram acquisitions are triggered when the moving mirror has moved by a distance corresponding to an integer multiple of HeNe wavelength (λ_{HeNe}). Another technical term widely used to describe this concept is “sampling distance”. Figure 13 depicts a particular case where the acquisition is triggered at each λ_{HeNe} which yields a sampling distance of 1. For clarity and visualization purposes, the interferograms shown on the figure are not to scale.

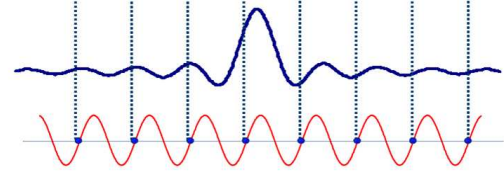


Figure 13. Acquisition triggering at each λ_{HeNe} (sampling distance of $1 \lambda_{\text{HeNe}}$)

Table 1. Sampling periods for FIRST series spectral bands

Spectral band	Wavenumber range [cm ⁻¹]	Minimum sampling frequency [cm ⁻¹]	Maximum sampling distance [n × λ _{HeNe}]
MW-E	2000 – 6667	13 333	1
MW	2000 – 3333	6667	2
LW	909 – 1250	2500	6

The HeNe laser emits at a wavelength of 632.8nm (or a wavenumber of 15 800 cm⁻¹). Nyquist’s criterion states that the sampling frequency (in wavenumber for this application) must be at least twice the highest frequency measured by the instrument. Table 1 summarizes the maximum sampling distance for each spectral band that the FIRST series can cover. It can also be seen in this table that when data is acquired at shorter wavelengths (or, equivalently, at higher wavenumbers), the sampling distance must be shorter.

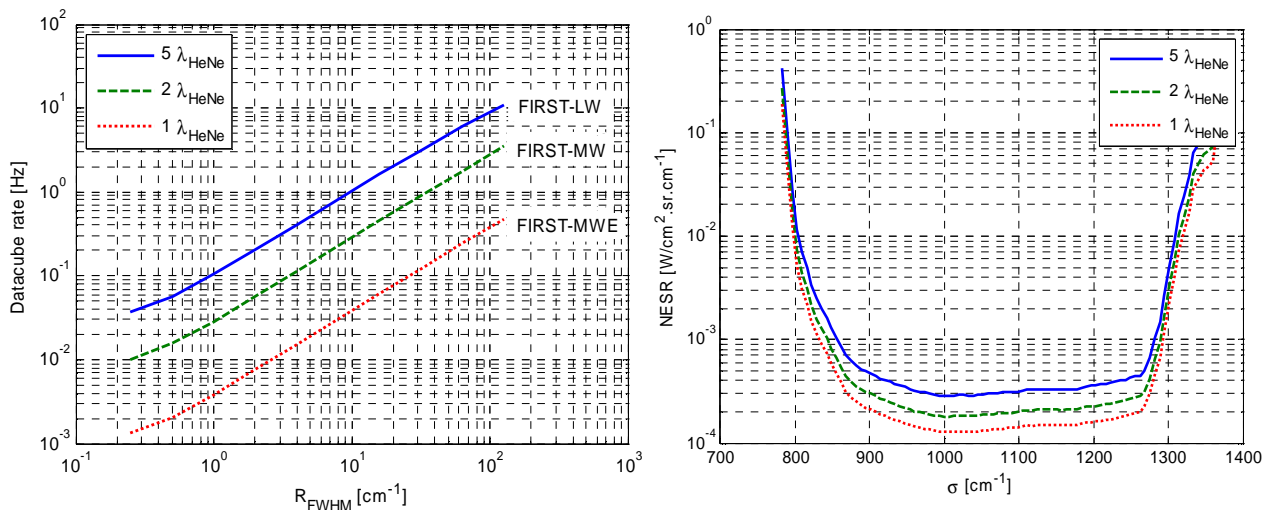


Figure 14. Left-hand side: Effect of sampling distance on datacube rate and spectral resolution Right-hand side: Effect of sampling distance on NESR

The bottleneck of FIRST acquisition rate is its FPA frame rate which suggests that increasing the number of measured points directly affects the datacube rate. This assertion is illustrated on the left-hand side of Figure 14 where the datacube rate is plotted as a function of spectral resolution for different sampling distances. As was mentioned before, for a fixed datacube rate, spectral resolution is dependant on the sampling period. For a given data cube rate, the best spectral resolution performances are obtained with the FIRST-LW because Nyquist's criterion is easier to meet with instruments that acquire data at lower wavenumbers.

The NESR curves seen on the right-hand side of Figure 14 clearly demonstrate that this performance criterion is also affected by the interferogram sampling distance. This is explained by two different factors. Firstly, it was demonstrated that datacube rates increase for higher sampling distances. Therefore, the total measurement time is shorter and equation 2 then states that NESR will increase. Secondly, if it is assumed that white noise is present in the interferogram, then, according to Parseval's theorem, the total noise is redistributed over all spectral bins after application of the FFT algorithm. Hence, if there are more points in the interferogram (and consequently more points in the resulting spectrum), a smaller portion of the total noise is present at each wavenumber. Smaller sampling distances thus result in better NESR.

These observations underline the trade that must be performed between spectral resolution, NESR and temporal resolution in the airborne configuration.

4.6 Impact of aircraft altitude

In addition to the inherent dependency of spatial resolution and ground area coverage on altitude, spectral resolution is also collaterally affected by this flight condition. Indeed, the aircraft displacement is compensated by the IMC mirror so that the instrument observes the same location on the ground for the entire duration of a datacube acquisition. The FIRST-airborne IMC mirror angular range is restricted to $\pm 1.1^\circ$ in order to avoid exaggerated deformation of the pixel shape projected on the ground (see Section 3.1). As Figure 15 illustrates, when the aircraft is flying at lower altitudes, the IMC mirror must scan the scene faster and it thus reaches its angular limits earlier than at higher altitudes. Hence, the available sweep time to collect data is smaller and, as a result, the spectral resolution is lower.

The interdependency amongst spectral resolution, aircraft altitude and spatial resolution is plotted in Figure 16 for both the FIRST-LW and FIRST-MW sensors. As expected, we notice that the spectral resolution is inversely proportional to both altitude and spatial resolution. Moreover, it is once again evident that in order to achieve the best spectral resolution it is preferable to use the longest possible sampling distance but, as usual, this is accomplished at the expense of NESR performances.

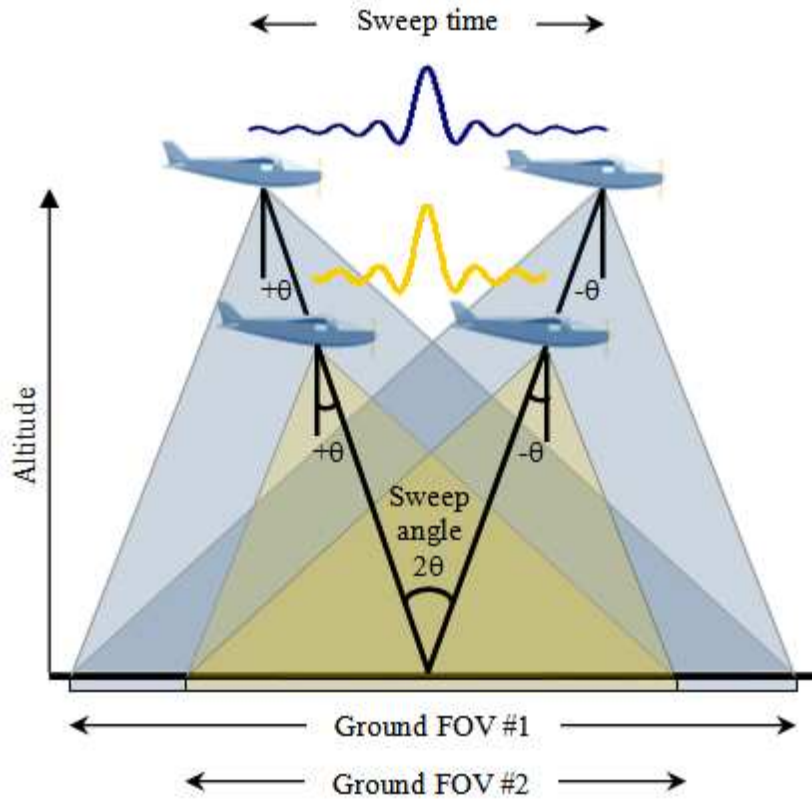


Figure 15. Impacts of altitude on performances

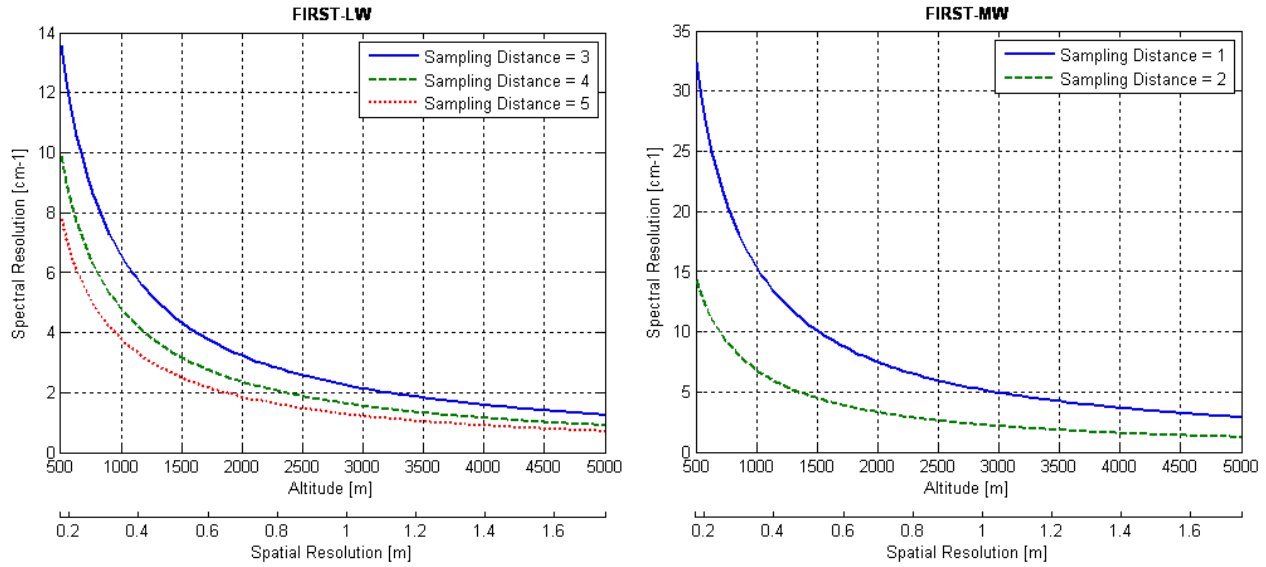


Figure 16. Best achievable spectral resolution in function of aircraft altitude and spatial resolution

For the highest altitude (5000 m), Table 2 indicates the best achievable spectral resolution for each instrument configuration.

Table 2. Best performance at an altitude of 5000 m

Spectral band	Best spectral resolution [cm ⁻¹]
MW-E	5
MW	2.25
LW	0.35

4.7 Impact of aircraft speed

The best spectral performances are associated with lower aircraft speeds since the FIRST-airborne then has more time to acquire data over a same ground area and it can thus be operated at higher spectral or spatial resolutions or with better NESR values. Figure 17, illustrates the effect on the spectral resolution of a 20 m/s speed variation for the FIRST-LW sensor. On the left-hand and right-hand side images, the aircraft speed is respectively 50 m/s and 70 m/s. These curves show that a 30 percent speed decrease results in a spectral resolution improvement of 150% to 300% (depending on the sampling period being used). It is to be noted that if the selected overlap (in this case 10%) between two datacubes or the swath width (here, 64 pixels) are changed, the impacts of the aircraft speed might differ from what is seen on Figure 17.

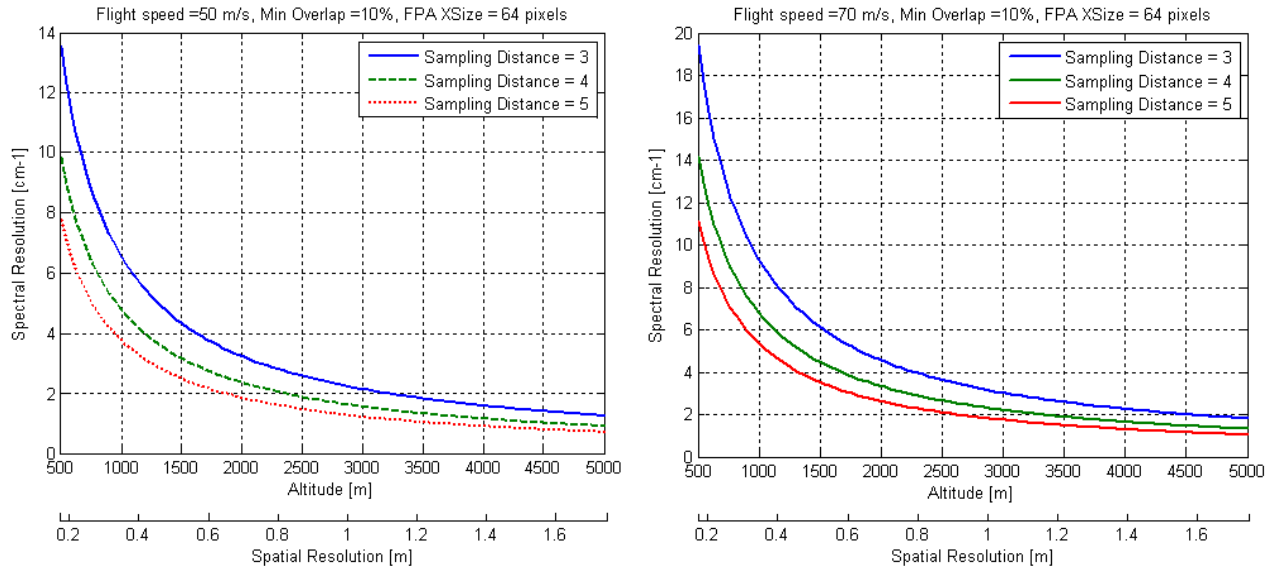


Figure 17. Effect of aircraft speed on spectral resolution. The sampling distances are in units of multiples of HeNe wavelengths.

4.8 Impact of spatial windowing

It was mentioned that the FPA frame rate is a limiting factor for the sweep time and, consequently, it is also for the spectral resolution. The frame rate can be increased by outputting fewer pixels from the camera. This action is sometimes referred to as spatial windowing. Spatial windowing constitutes an elegant way of increasing the achievable spectral resolution limit.

Along the flight path, the number of pixels is selected between 4 and 256 pixels to optimize spectral resolution and NESR for a given aircraft speed and altitude.

On the other hand, the swath width defined as the number of selected pixels in the dimension perpendicular to the flight direction, can be modified to increase the FPA frame rate. Examples of narrow and wide swath widths are illustrated in Figure 18. Reducing the swath width obviously affects the ground area covered by the instrument. It thus requires more flight lines to cover a given ground surface. This is why the default swath width value in the mission planner software is always set to 320 pixels (the maximum number of pixels in this dimension). However, if one wishes to improve spectral resolution, the swath width can be narrowed down to a minimum of 64 pixels. At lesser swath widths, the FPA performs spatial cropping, and no gain in performance is obtained.

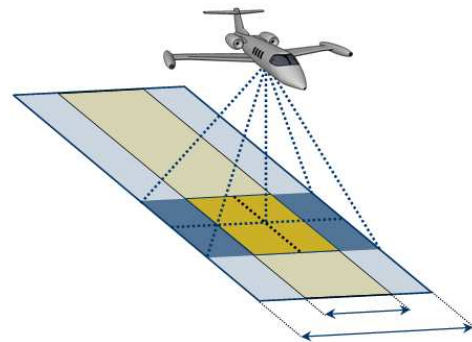


Figure 18. Examples of narrow and wide swath widths

In Figure 19, the spectral resolution is plotted for different swath widths as a function of altitude and spatial resolution. It is seen that, for all altitudes, narrowing the swath width always improves the achievable spectral resolution. This graph also shows that, for a given swath width, the best achievable spectral resolution converges towards a constant value as higher altitudes are reached. This behavior is explained by the fact that the number of pixels in the direction of propagation of the aircraft is adjusted automatically to optimize spectral resolution. The inflexion point occurs at the lowest altitude where it is no longer possible to decrease the number of pixels along the flight path in order to maintain the same spectral resolution.

In Figure 19, the spectral resolution is plotted for different swath widths as a function of altitude and spatial resolution. It is seen that, for all altitudes, narrowing the swath width always improves the achievable spectral resolution. This graph also shows that, for a given swath width, the best achievable spectral resolution converges towards a constant value as

higher altitudes are reached. This behavior is explained by the fact that the number of pixels in the direction of propagation of the aircraft is adjusted automatically to optimize spectral resolution.

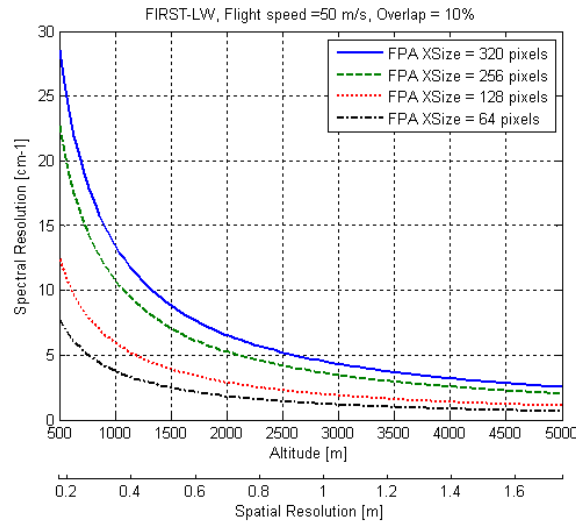


Figure 19. Effect of Swath Width on Spectral Resolution

5. CONCLUSION

This paper reported on the analysis and development of the FIRST-airborne, a hyperpectral imaging airborne system based on FTS technology. The module includes two hyperspectral imagers covering the MW and LW parts of the electromagnetic spectrum. To maximize the performances of the instrument, an image motion compensation scheme and a stabilization platform are also included. A GPS-INS is integrated in the system to enable ortho-rectification and geo-referencing of the collected data.

The FIRST instruments offer uncommon flexibility in adjusting their spatial, spectral and temporal parameters. This flexibility proves to be invaluable for airborne applications where the flight parameters impose severe restrictions on spectrometer operation. Optimized performances in terms of spatial resolution, spectral resolution and NESR can thus be obtained and tuned according to user requirements. The relationship amongst all of these criteria was studied and presented in this paper. It is concluded that, for a given aircraft altitude and speed, the instrument settings must be carefully selected to optimize performances. The user is helped in this process by the dedicated mission planning tool developed for the FIRST-airborne system.

The FIRST-airborne will soon enter in its experimental testing phase. The next mission will include collecting data of gas releases as well as UXOs measurements. Telops is also studying the feasibility of integrating the FIRST-airborne on other types of aircrafts such as helicopters and unmanned aerial vehicles.

REFERENCES

1. Alexandre Vallières, André Villemaire, Martin Chamberland, Louis Belhumeur, Vincent Farley, Jean Giroux and Jean-François Legault, Algorithms For Chemical Detection, Identification And Quantification For Thermal Hyperspectral Imagers, Proc. SPIE Vol. 5995, p. 147-157, Chemical and Biological Standoff Detection III, Jensen, James O. Thériault, Jean-Marc, Ed., November 2005.
2. Vincent Farley, Martin Chamberland, Philippe Lagueur, Alexandre Vallières, André Villemaire and Jean Giroux, Chemical Agent Detection and Identification with a Hyperspectral Imaging Infrared Sensor, Proc. SPIE Vol. 6661, p. , Imaging Spectrometry XII, Sylvia S. Shen, Paul E. Lewis, Ed., September 2007.